Fast Quantum State Preparation and Bath Dynamics Using Non-Gaussian Variational *Ansatz* and Quantum Optimal Control

Liam J. Bond,[1,2] Arghavan Safavi-Naini,[1,2] and Jiří Minář[3,1,2]
[1]*Institute for Theoretical Physics, Institute of Physics, University of Amsterdam, Science Park 904, 1098 XH Amsterdam, The Netherlands*
[2]*QuSoft, Science Park 123, 1098 XG Amsterdam, The Netherlands*
[3]*CWI, Science Park 904, 1098 XH Amsterdam, The Netherlands*

(Received 23 June 2023; revised 15 January 2024; accepted 25 March 2024; published 23 April 2024)

Fast preparation of quantum many-body states is essential for myriad quantum algorithms and metrological applications. Here, we develop a new pathway for fast, nonadiabatic preparation of quantum many-body states that combines quantum optimal control with a variational *Ansatz* based on non-Gaussian states. We demonstrate our approach on the spin-boson model, a single spin interacting with the bath. We use a multipolaron *Ansatz* to prepare near-critical ground states. For one mode, we achieve a reduction in infidelity of up to ≈60 (≈10) times compared to linear (optimized local adiabatic) ramps; for many modes, we achieve a reduction in infidelity of up to ≈5 times compared to nonadiabatic linear ramps. Further, we show that the typical control quantity, the leakage from the variational manifold, provides only a loose bound on the state's fidelity. Instead, in analogy to the bond dimension of matrix product states, we suggest a controlled convergence criterion based on the number of polarons. Finally, motivated by the possibility of realizations in trapped ions, we study the dynamics of a system with bath properties going beyond the paradigm of (sub- and/or super-) Ohmic couplings.

DOI: 10.1103/PhysRevLett.132.170401

Introduction.—The description of quantum systems out of equilibrium represents a notorious challenge. In many relevant situations one has to resort to numerical approaches ranging from nonequilibrium Monte Carlo to tensor networks [1–10]. A specific class of problems consists of systems containing bosonic degrees of freedom with an (even locally) unbounded Hilbert space. To deal with such situations, various schemes have been devised, such as path integral techniques [11–14] or effective Hamiltonian [15,16] and light cone conformal truncation [17–19] used predominantly in high-energy physics, which aim at describing the relevant part of the (bosonic) Hilbert space by a suitable choice of truncation procedure.

Another possibility is to exploit the continuous-variable structure of the bosonic states. Here, a novel scheme using a time-dependent variational *Ansatz* based on *non-Gaussian* states has been recently proposed [20,21] and successfully applied to the studies of systems ranging from the Kondo impurity problem [22], central spin [23], or spin-Holstein models [24] to Bose and Fermi polarons [25–27].

In this Letter, we demonstrate that non-Gaussian *Ansätze* constitute a natural framework to study physics in non-perturbative regimes and propose a novel approach to quantum many-body state preparation by combining quantum optimal control and non-Gaussian variational *Ansätze* [28–31]. Specifically, we implement a multipolaron *Ansatz* [32–38] and extend previous studies of the paradigmatic (sub- and/or super-)Ohmic spin-boson model [11–14,39–44] to in principle arbitrary couplings. The choice of the spin-boson model is motivated by the fact that it plays a major role in the description of impurity problems, while also encompassing many platforms that are currently used for quantum simulation and computing, ranging from superconducting circuits to trapped ions [45–59]. In particular, recent realizations of the quantum Rabi-Hubbard [60] and Rabi models [61,62] represent an ideal test bed to experimentally probe the here-presented theoretical results.

We study (i) the convergence of the multipolaron *Ansatz*, highlighting the limitations of the leakage as a control parameter and instead proposing a quantifiable measure of convergence based on the number of polarons, (ii) the onset of chaos of the bosonic bath quantified by the out-of-time-order correlators (OTOCs), demonstrating its robustness with respect to the spin-bath couplings, and (iii) fast nonadiabatic quantum many-body state preparation, including the preparation of near-critical ground states.

The model.—We consider the spin-boson model, where the interaction of a two-level system with a bath of N harmonic oscillators is described by the Hamiltonian

$$H = \frac{\Delta}{2}\sigma_x + \sum_{k=1}^{N} \epsilon_k b_k^\dagger b_k - \frac{1}{2}\sigma_z \sum_{k=1}^{N} g_k (b_k^\dagger + b_k). \quad (1)$$

Here Δ describes the tunneling strength, ϵ_k is the mode frequency, and g_k is the interaction between the spin and

kth mode. The operators $\sigma_{x,y,z}$ are Pauli operators acting on the spin, and b_k ($b_k^\dagger$) are the annihilation (creation) operators of the bath modes satisfying $[b_k, b_{k'}^\dagger] = \delta_{kk'}$. The Hamiltonian (1) conserves the parity $P_{\mathrm{ex}} = e^{i\pi N_{\mathrm{ex}}}$, where $N_{\mathrm{ex}} = 1/2(\sigma_x + 1) + \sum_k b_k^\dagger b_k$ counts the total number of excitations.

Typically the spin-boson model is studied with an Ohmic ($s = 1$), sub-Ohmic ($s < 1$), or super-Ohmic ($s > 1$) bath, with the couplings described by $\sum_k g_k^2 \delta(\omega - \epsilon_k) = 2\alpha\omega_c^{1-s}\omega^s\Theta(\omega_c - \omega)$. Here $\omega > 0$, ω_c is a high-frequency cutoff, and α is a dimensionless measure of the spin-bath interaction strength. We choose a mode discretization $\epsilon_k = \omega_c k/N$, $k = 1, 2, \ldots, N$. Note that we do not enforce any restrictions on any of the relevant energy scales, i.e., Δ, ϵ_k, g_k, or ω_c. In particular, we do not require that ω_c is the largest energy scale. Such tunability is motivated by the possibility of realizing the spin-boson model with tunable parameters in trapped ions [63].

Time-dependent variational principle with non-Gaussian states.—We consider a variational state $|\psi(\vec{x})\rangle$ parametrized by a set of real parameters $\vec{x}(t)$. Using the variational principle, the imaginary and real-time evolution are governed by the equations of motion [20,21,63]

$$\dot{x}^\nu = -(g_{\mu\nu})^{-1}\partial_\mu \epsilon(\vec{x}, t), \tag{2a}$$

$$\dot{x}^\nu = -(\omega_{\mu\nu})^{-1}\partial_\mu E(\vec{x}, t). \tag{2b}$$

Here $\epsilon(\vec{x}, t) = E(\vec{x}, t)/\langle\psi(\vec{x})|\psi(\vec{x})\rangle$, $E(\vec{x}, t) = \langle\psi(\vec{x})|H(t)|\psi(\vec{x})\rangle$, $g_{\mu\nu} = 2\mathrm{Re}\langle v_\mu|v_\nu\rangle$, and $\omega_{\mu\nu} = 2\mathrm{Im}\langle v_\mu|v_\nu\rangle$ with $|v_\mu\rangle = \partial_\mu|\psi(\vec{x})\rangle$ the tangent vectors of the variational manifold and $\partial_\mu = \partial/\partial x^\mu$ [63]. We use (2a) and (2b) to access the ground state in the $\tau \to \infty$ limit of imaginary time and to calculate real-time dynamics, respectively.

The crucial input to the equations of motion is an *Ansatz* for the wave function, which we choose to be a weighted superposition of coherent states,

$$|\psi(\vec{x})\rangle = \sum_{p=1}^{N_p} D_p^{(\uparrow)}|\uparrow, 0\rangle + D_p^{(\downarrow)}|\downarrow, 0\rangle, \tag{3}$$

where $D_p^{(\uparrow,\downarrow)} = e^{\kappa + i\theta}\mathcal{D}(\vec{\alpha})$, $\mathcal{D}(\vec{\alpha}) = \prod_{k=1}^N \exp[\alpha_k b_k^\dagger - \alpha_k^* b_k]$ is the standard displacement operator of the bosonic modes and κ, θ encode the respective weights. Here $\vec{\alpha} = (\alpha_1, \ldots, \alpha_N)$, and we have dropped the $p, \uparrow, \downarrow$ indices for ease of notation.

Because the set of coherent states forms an overcomplete basis for the N-mode bosonic Hilbert space, in the limit $N_p \to \infty$ the multipolaron *Ansatz* becomes exact. When $N_p = 1$, the bosonic part in each spin sector reduces to a coherent state, a special case of a Gaussian state. We comment on the intuition behind the suitability of the multipolaron *Ansatz* for the spin-boson model and the role of squeezing in Supplemental Material [63].

The *Ansatz* (3) whose evolution is governed by Eqs. (2) is an example of time-dependent variational principle. It has recently found numerous applications to the time evolution of spin systems, where it is often formulated as a tensor network with time-dependent parameters [77–82]. Typically, the quality of the *Ansatz*'s evolution is quantified by a leakage

$$\Lambda(t) = \|(\partial_t + iH(t))|\psi(\vec{x})\rangle\|, \tag{4}$$

which measures the rate at which the *Ansatz* wave function leaves the variational manifold under the action of the Hamiltonian $H(t)$. From the leakage, the fidelity of the *Ansatz* with respect to the true state $|\Psi(t)\rangle$ at time t can be bounded by [80]

$$\mathcal{F}(t) = |\langle\Psi(t)|\psi(\vec{x})\rangle|^2 \geq \left(1 - \frac{[\int_0^t \mathrm{d}\tau\Lambda(\tau)]^2}{2}\right)^2. \tag{5}$$

Results.—First, we benchmark the performance of the *Ansatz* (3) by considering the Hamiltonian (1) with a single mode, also known as the quantum Rabi model (QRM). In this case the Ohmic coupling reduces to $g = \sqrt{2\alpha}\epsilon$ (with $\omega_c = \epsilon$), so we use g and α interchangeably. The QRM features a crossover from a bi- to quadpolaron state at the critical coupling strength $g_c = 2\sqrt{\epsilon^2 + \sqrt{\epsilon^4 + (g_{c0}/2)^4}}$. In the so-called thermodynamic limit $\Delta/\epsilon \to \infty$ the crossover corresponds to a quantum phase transition from a normal to a superradiant phase at $g_{c0} = \sqrt{\epsilon\Delta}$ [83,84].

In Figs. 1(a) and 1(b) we show the order parameter $\langle\sigma_x\rangle$ of the ground state in the vicinity of the crossover and the real-time dynamics for a quench from an initial state $|\psi(t = 0)\rangle = |0\rangle|+\rangle$. We see a fast convergence to the exact diagonalization (ED) results for a moderate polaron number N_p. The respective fidelities (5) are then shown in Figs. 1(c) and 1(d).

The dotted lines in Fig. 1(d) show the fidelity bound from the right-hand side of Eq. (5). The bound appears to be relatively loose in that it overestimates the actual decay of the fidelity. Although the leakage provides at least some control over the accuracy of a given *Ansatz*, the multipolaron state (3) has the advantage that it offers the number of polarons as a control parameter. In particular, $|\psi(t)\rangle \to |\Psi(t)\rangle$ in the limit $N_p \to \infty$. As such, considering the real-time dynamics of an observable $\mathcal{O}$, we introduce a convergence criterion

$$(\Delta\mathcal{O}/\bar{\mathcal{O}})^{(N_p)}(T) = \frac{\int_0^T \mathrm{d}t|\mathcal{O}^{(\max[N_p])}(t) - \mathcal{O}^{(N_p)}(t)|}{|\int_0^T \mathrm{d}t\mathcal{O}^{(N_p)}(t)|}, \tag{6}$$

which quantifies the relative (time-integrated) change in the evolution of the observable with respect to the maximum

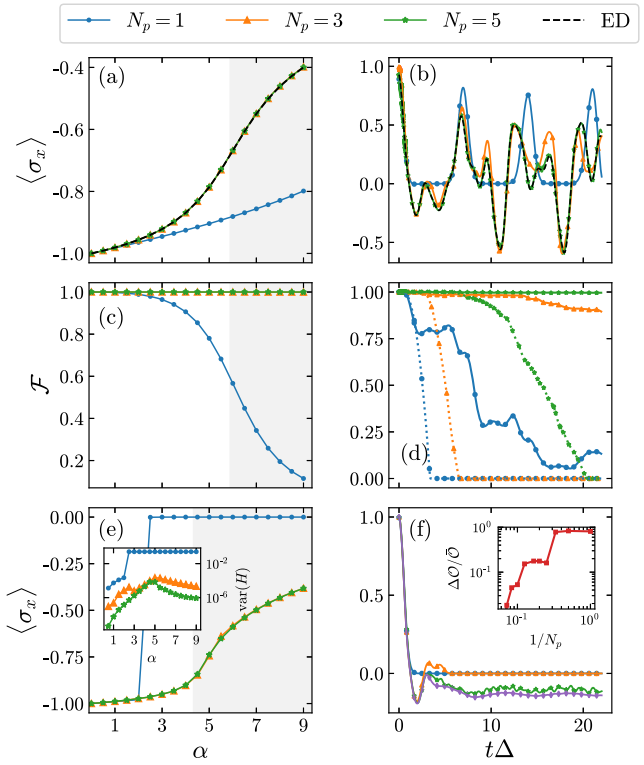

FIG. 1. Single mode: (a) Order parameter $\langle\sigma_x\rangle$ of the $P_{\mathrm{ex}} = 1$ ground state and (c) fidelity $\mathcal{F} = |\langle\Psi_{\mathrm{gs}}|\psi_{\mathrm{gs}}\rangle|^2$ for $\epsilon/\Delta = 0.15/1.0$. The white and gray regions indicate the phase boundary between the normal and superradiant phase in the thermodynamic limit with the critical point $g_c = \sqrt{\epsilon\Delta}$. (b) Time evolution of $\langle\sigma_x\rangle$ from initial state $|0\rangle|+\rangle$ for $\epsilon/\Delta = 1.0/1.1$, $g/\Delta = 2.0/1.1$. (d) The fidelity $\mathcal{F} = |\langle\Psi(t)|\psi(t)\rangle|^2$ (solid) with the lower bound obtained from the leakage (dotted), cf. Eq. (5). Many modes: (e) Order parameter $\langle\sigma_x\rangle$ for $N = 10$ modes. For illustration, we also include the perturbative result with critical point $\alpha_c \approx 1 + \Delta/2\omega_c$ separating the delocalized (white) and localized (gray) phases [39,41]. The inset plots var(H), which is largest near α_c due to the absence of squeezing in the *Ansatz*. (f) Real-time dynamics from initial state $|0\rangle|+\rangle$, with the purple line $N_p = 16$. Parameters are $\omega_c/\Delta = 1.0/1.1$ and $\alpha = 4.0$.

considered number of polarons N_p. Here $\mathcal{O}^{(N_p)}(t) = \langle\psi(t)|O|\psi(t)\rangle$ is the expectation value obtained with N_p polarons. We note that similar convergence criteria have been discussed in Refs. [35,36].

With these definitions at hand, we return to the Ohmic spin-boson Hamiltonian (1) to plot ground state properties and real-time dynamics for $N = 10$ modes, shown in Figs. 1(e) and 1(f), respectively. The inset of Fig. 1(e) plots $\mathrm{var}(H) = \langle H^2\rangle - \langle H\rangle^2$, which we use as a control quantity of the *Ansatz* as $\mathrm{var}(H) = 0$ for the ground state. We see rapid improvement for $N_p > 1$, with relatively worse performance near the critical point $\alpha_c \approx 5$. This is expected because our *Ansatz* does not include squeezing, which is a property of the ground state near the critical point [84]. In the inset of Fig. 1(f), we plot $(\Delta\mathcal{O}/\bar{\mathcal{O}})^{(N_p)}(T)$ for $\mathcal{O} = \sigma_x$. We find $N_p > 5$ sufficient to accurately capture real-time dynamics, with $N_p > 10$ highly accurate.

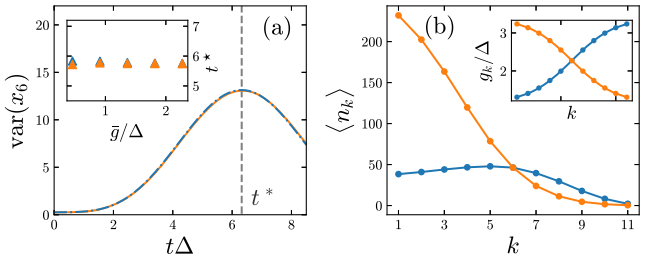

FIG. 2. (a) Bath-mode position quadrature of the mid-k ($k = 6$) mode for a quench from a state $|\psi(t = 0)\rangle = |0\rangle|+\rangle$ for the coupling profiles g_k^+ (blue, dashed) and g_k^- (orange, solid), see Eq. (7) and the inset in (b). The vertical dashed line indicates the scrambling time t^* corresponding to the first maximum of var(x_6). The inset shows t^* vs coupling amplitude $\bar{g}$ for the two profiles. (b) The occupation of the bath modes at the scrambling time. Parameters are $\omega_c/\Delta = 1/1.1$, $\bar{g}/\Delta = 1/1.1$ and $N = 11$, $N_p = 10$.

Bath dynamics.—The *Ansatz* (3) can be used to further quantify the bath dynamics. To this end, we evaluate the fidelity OTOC, $F = \langle W^\dagger(t)V^\dagger W(t)V\rangle$ with $V = |\psi(0)\rangle\langle\psi(0)|$ the projector on the initial state and $W = \exp(i\delta\phi G)$ [85–87]. For a small perturbation $\delta\phi \ll 1$, $1 - \mathcal{F} \propto \mathrm{var}(G)$. We choose $G = x_k = b_k^\dagger + b_k$, the position quadrature of the kth mode. Such fidelity OTOCs have been considered in the analysis of chaos in the QRM in Ref. [64], where it was found that the scrambling time t^* corresponding to the maximum of var(x) in the superradiant phase and for a quench from a vacuum depends only weakly on the exact value of the coupling g in the thermodynamic limit $\Delta/\varepsilon \to \infty$.

We demonstrate the versatility of the *Ansatz* by moving beyond the paradigm of Ohmic-type baths. We consider a set of equally spaced k modes with coupling profiles

$$g_k^\pm = \frac{\bar{g}}{2}\tanh[\pm 0.25(k - \lceil N/2\rceil)] + \bar{g}, \tag{7}$$

as shown in the inset of Fig. 2(b). In Supplemental Material [63] we investigate the convergence of the *Ansatz* with polaron number N_p for a variety of bath profiles including sub- and super-Ohmic ones. Here, we study quench dynamics for both $g_k^\pm$ from $|\psi(t = 0)\rangle = |0\rangle|+\rangle$ for $N = 11$ modes far from the thermodynamic limit with $\Delta/\omega_c = 1.1$. In Fig. 2(a) we show the variance var(x_6) of the midcoupling (sixth) mode with the scrambling time t^* indicated. The inset shows the dependence of t^* as a function of the coupling strength amplitude $\bar{g}$ (here all the couplings correspond to the (pseudo) coherent dynamics in the phase diagram [63]) and the corresponding bosonic excitation number distribution at t^* is shown in Fig. 2(b). We find that the weak dependence of t^* from the QRM in the superradiant phase and thermodynamic limit seems to be a robust

feature that persists in the many-mode case with very different coupling profiles and far from perturbative limits [63]. We leave this interesting opening for future systematic investigations and turn to the application of the *Ansatz* to fast quantum state preparation.

Quantum optimal control.—Adiabatic quantum state preparation, where the Hamiltonian parameters are changed such that the state during time evolution corresponds to the instantaneous ground state, is an often-employed and established paradigm with many applications. A prototypical example where this scheme fails is the preparation of critical states, as the adiabatic criterion cannot be satisfied due to the closure of the gap [88]. Going beyond adiabatic schemes requires the design of ramp protocols that generate a dynamical trajectory that takes the initial state to the target final state. Both determining the critical ground state and designing nonadiabatic ramp protocols can be challenging for systems with many bosonic modes.

The variational principle, which casts both the real and imaginary time evolution in the form of first order differential equations (2) for the variational parameters, offers an ideal setup to implement such ramp protocols with quantum optimal control methods.

We consider the chopped-random basis protocol (CRAB) [29,90], an optimization technique that optimizes the ramp of a control parameter by applying corrections in the form of a truncated Fourier decomposition. A CRAB-optimized ramp protocol can be nonadiabatic, and thus its speed is not limited by the gap. Let us first consider the quantum Rabi model. In analogy to the preparation of ground states by tuning the coupling g [62,65], we consider $g(t) = g_f t/t_f f(t)$, where g_f is the target coupling determining the corresponding ground state and where $f(t)$ is a Fourier decomposition into M harmonics,

$$f(t) = \frac{1}{\mathcal{N}}\left[1 + \sum_{j=1}^{M} A_j \sin(\nu_j t) + B_j \cos(\nu_j t)\right]. \quad (8)$$

Here $\mathcal{N} = 1 + \sum_j B_j$ is a normalization factor that ensures $g(t_f) = g_f$, $\nu_j = 2\pi j(1 + r_j)/t_f$, $r_j \in \{0, 1\}$ are random integers, and the coefficients A_j, B_j are the optimization parameters. Using random numbers and repeating the optimization several times avoids the need to include r_j as optimization parameters, while still enabling a large parameter search area and fast convergence [91].

To assess the performance of the protocol, we prepare a target ground state in the vicinity of the crossover (phase transition), which is located at coupling g_c. Specifically, we evaluate the preparation time t_f needed to prepare the target state with a fidelity $\mathcal{F} > 0.99$. For comparison, we also consider a linear ramp protocol $g(t) = g_f t/t_f$ and a local adiabatic (LA) ramp obtained by solving the differential equation $\gamma = |\Delta^2(g)/\dot{g}(t)|$, where $\Delta(g)$ is the instantaneous energy gap between the ground and first coupled excited

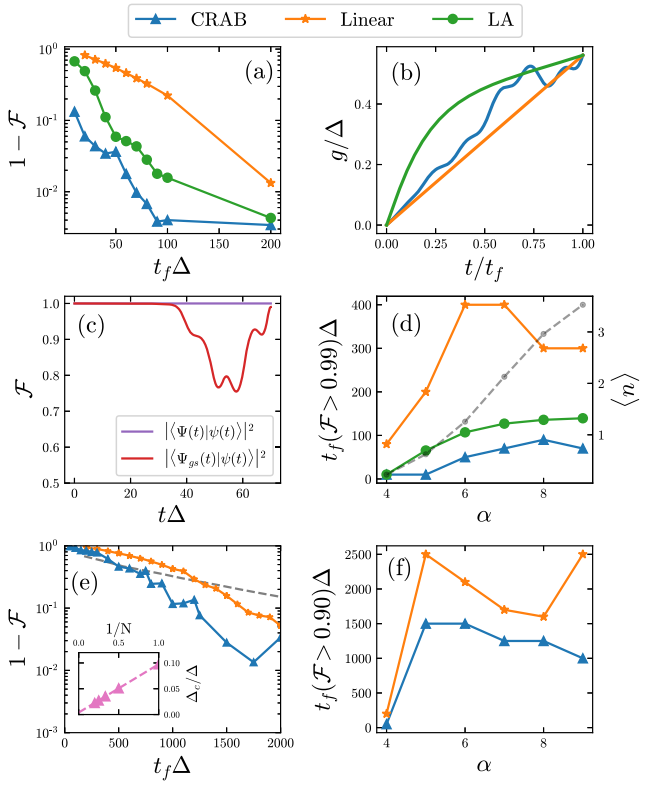

FIG. 3. Single mode: (a) The infidelity $1-\mathcal{F}$, $\mathcal{F} = |\langle\psi_{\rm gs}|\psi(t_f)\rangle|^2$, where $|\psi_{\rm gs}\rangle$ is the target ground state with $\alpha = 7$, and $|\psi(t_f)\rangle$ is the state prepared with CRAB, linear, and LA ramps. An example of the three ramps for $t_f = 70$ is shown in (b). In (c) we verify the accuracy of the CRAB simulation (purple) and its nonadiabaticity (red) by computing the overlap with the instantaneous ground state $|\Psi_{\rm gs}(t)\rangle$. (d) Minimum ramp times required to prepare a target ground state at α with fidelity $\mathcal{F} > 0.99$. The right axis shows the ground state boson number (gray dashed line). Many modes: (e) Infidelity for CRAB and linear ramp protocols vs ramp time for $N = 10$ modes with finite-size scaling of the minimum gap (inset). For comparison we show the gray dashed line obtained by extrapolating the linear ramp data from (a), see Supplemental Material [63]. (f) Ramp times required to prepare the target state with fidelity $\mathcal{F} > 0.90$ vs α, see text for details. Parameters used, $N_p = 5$, $\omega_c/\Delta = 0.15$.

state, and $\gamma \gg 1$ is an adiabaticity parameter [66,92]. In Fig. 3(a), we plot the infidelity as a function of the preparation time for the CRAB, linear, and LA ramp protocols. The corresponding time profiles of the couplings $g(t)$ are shown in Fig. 3(b). For a set t_f the CRAB protocol offers a significant reduction in infidelity of ≈60 times and ≈10 times compared to linear and optimized adiabatic ramps, respectively. To verify that the CRAB optimization does not correspond to adiabatic evolution, in Fig. 3(c) we show the overlap $|\langle\Psi_{\rm gs}(t)|\psi(t)\rangle|^2$ of the variational state with the instantaneous ground state $|\Psi_{\rm gs}(t)\rangle$ [we also verify that the variational state corresponds to the exact evolution $|\langle\Psi(t)|\psi(t)\rangle|^2 \approx 1$]. In Fig. 3(d) we show the extracted

preparation times for the three protocols as a function of the coupling together with the ground state boson number (gray dashed). We see that the CRAB optimization clearly outperforms both the linear and the LA ramp protocols: up to ≈10 times and ≈2 times faster than linear and optimized adiabatic ramps, respectively.

Moving to the many-mode case, we consider $N = 10$ modes with Ohmic couplings. The target ground state for each α is determined using the imaginary time evolution (2a). The infidelity for a given ramp time t_f for the linear and CRAB protocols is shown in Fig. 3(e) (we omit the LA ramp for simplicity [63]). The inset shows the finite-size scaling of the gap [93]. The gray dashed line, obtained by extrapolating the data for $\mathcal{F} = 0.9$ from Fig. 3(a) and using the scaled gap, is shown for comparison [63].

Next, we consider the target fidelity $\mathcal{F} > 0.9$, as very high target fidelities are more stringent on the quality of the approximation (requiring sufficiently large N_p), cf. Figs. 1(f). Figure 3(f) shows the preparation times t_f vs α. Here, the adiabaticity parameter $\gamma = O(1)$ [63], which indicates that the linear ramp times result in nonadiabatic evolution, which here is sufficient to reach the target $\mathcal{F} = 0.9$ with only a mild improvement factor ≈2 in the preparation times using the CRAB protocol [63]. This should be contrasted with $\gamma \approx$ 10–20 in Fig. 3(d) resulting in higher improvement factor of ≈10 using the CRAB protocol.

Outlook.—We have demonstrated the application of a multipolaron non-Gaussian variational *Ansatz* to study bath dynamics beyond (sub- and/or super-)Ohmic couplings and combined it with quantum optimal control for fast quantum state preparation. As next steps, it would be interesting to investigate the bath dynamics in such nonperturbative setting including entanglement growth between the bath modes mediated by the spin or the possible absence of bound on OTOCs in such a star-graph-like configuration [94], targeting experimental verification with trapped ions [61,62]. Another straightforward extension of our analysis is the computation of the gap through linear response [20,21] and considering carrier ramp profiles beyond the linear one, such as the LA profile in Fig. 3(b). This is likely to further reduce the state preparation times. Remarkably, already the simpler Gaussian version of the *Ansatz* [95] allows for efficient description of systems in higher dimensions [96] or to extract scaling exponents at the phase transition [97].

Finally, we note that there are intense efforts underway to use the bosonic degrees of freedom in noisy intermediate-scale quantum devices, particularly trapped ions, for quantum computing, quantum chemistry, and quantum error correction [98–102]. Such approaches require robust bosonic state preparation. In this context, it would be interesting to extend the combination of non-Gaussian states with quantum optimal control to a larger class of systems, including open dynamics [103–108], and to potentially embed it within hybrid classical-quantum variational approaches [99,100,109].

We would like to acknowledge stimulating discussions with D. Abanin, J. D. Bancal, E. Di Salvo, J. Home, M. Lewenstein, K. Schoutens, D. Schuricht, and W. Waalewijn. This work is supported by the Dutch Research Council (NWO/OCW), as part of the Quantum Software Consortium program (Project No. 024.003.037).

[1] N. Makri and D. E. Makarov, Tensor propagator for iterative quantum time evolution of reduced density matrices. II. Numerical methodology, J. Chem. Phys. **102**, 4611 (1995).
[2] M. Thorwart, P. Reimann, P. Jung, and R. Fox, Quantum hysteresis and resonant tunneling in bistable systems, Chem. Phys. **235**, 61 (1998).
[3] M. Thorwart, P. Reimann, and P. Hänggi, Iterative algorithm versus analytic solutions of the parametrically driven dissipative quantum harmonic oscillator, Phys. Rev. E **62**, 5808 (2000).
[4] T. L. Schmidt, P. Werner, L. Mühlbacher, and A. Komnik, Transient dynamics of the Anderson impurity model out of equilibrium, Phys. Rev. B **78**, 235110 (2008).
[5] R. Orús, A practical introduction to tensor networks: Matrix product states and projected entangled pair states, Ann. Phys. (Amsterdam) **349**, 117 (2014).
[6] S. Montangero, S. Montangero, and Evenson, *Introduction to Tensor Network Methods* (Springer, New York, 2018).
[7] S. R. White and A. E. Feiguin, Real-time evolution using the density matrix renormalization group, Phys. Rev. Lett. **93**, 076401 (2004).
[8] P. Schmitteckert, Nonequilibrium electron transport using the density matrix renormalization group method, Phys. Rev. B **70**, 121302(R) (2004).
[9] M. Nuss, M. Ganahl, E. Arrigoni, W. von der Linden, and H. G. Evertz, Nonequilibrium spatiotemporal formation of the Kondo screening cloud on a lattice, Phys. Rev. B **91**, 085127 (2015).
[10] B. Dóra, M. A. Werner, and C. P. Moca, Information scrambling at an impurity quantum critical point, Phys. Rev. B **96**, 155116 (2017).
[11] P. Nalbach and M. Thorwart, Ultraslow quantum dynamics in a sub-Ohmic heat bath, Phys. Rev. B **81**, 054308 (2010).
[12] D. Kast and J. Ankerhold, Persistence of coherent quantum dynamics at strong dissipation, Phys. Rev. Lett. **110**, 010402 (2013).
[13] P. Nalbach and M. Thorwart, Crossover from coherent to incoherent quantum dynamics due to sub-Ohmic dephasing, Phys. Rev. B **87**, 014116 (2013).
[14] F. Otterpohl, P. Nalbach, and M. Thorwart, Hidden phase of the spin-boson model, Phys. Rev. Lett. **129**, 120406 (2022).
[15] D. Lee, N. Salwen, and D. Lee, The diagonalization of quantum field Hamiltonians, Phys. Lett. B **503**, 223 (2001).
[16] S. Rychkov and L. G. Vitale, Hamiltonian truncation study of the φ^4 theory in two dimensions, Phys. Rev. D **91**, 085011 (2015).

[17] N. Anand, A. L. Fitzpatrick, E. Katz, Z. U. Khandker, M. T. Walters, and Y. Xin, Introduction to light cone conformal truncation: QFT dynamics from CFT data, arXiv:2005.13544.
[18] H. Chen, A. L. Fitzpatrick, and D. Karateev, Bootstrapping 2d $\phi 4$ theory with Hamiltonian truncation data, J. High Energy Phys. 02 (2022) 146.
[19] L. V. Delacrétaz, A. L. Fitzpatrick, E. Katz, and M. T. Walters, Thermalization and chaos in a $1+1$d QFT, J. High Energy Phys. 02 (2023) 45.
[20] T. Shi, E. Demler, and J. Ignacio Cirac, Variational study of fermionic and bosonic systems with non-Gaussian states: Theory and applications, Ann. Phys. (Amsterdam) **390**, 245 (2018).
[21] L. Hackl, T. Guaita, T. Shi, J. Haegeman, E. Demler, and I. Cirac, Geometry of variational methods: Dynamics of closed quantum systems, SciPost Phys. **9**, 048 (2020).
[22] Y. Ashida, T. Shi, R. Schmidt, H. R. Sadeghpour, J. I. Cirac, and E. Demler, Efficient variational approach to dynamics of a spatially extended bosonic Kondo model, Phys. Rev. A **100**, 043618 (2019).
[23] Y. Ashida, T. Shi, R. Schmidt, H. R. Sadeghpour, J. I. Cirac, and E. Demler, Quantum Rydberg central spin model, Phys. Rev. Lett. **123**, 183001 (2019).
[24] J. Knörzer, T. Shi, E. Demler, and J. I. Cirac, Spin-Holstein models in trapped-ion systems, Phys. Rev. Lett. **128**, 120404 (2022).
[25] A. Christianen, J. I. Cirac, and R. Schmidt, Chemistry of a light impurity in a Bose-Einstein condensate, Phys. Rev. Lett. **128**, 183401 (2022).
[26] A. Christianen, J. I. Cirac, and R. Schmidt, Bose polaron and the Efimov effect: A Gaussian-state approach, Phys. Rev. A **105**, 053302 (2022).
[27] P. E. Dolgirev, Y.-F. Qu, M. B. Zvonarev, T. Shi, and E. Demler, Emergence of a sharp quantum collective mode in a one-dimensional Fermi polaron, Phys. Rev. X **11**, 041015 (2021).
[28] S. Lloyd and S. Montangero, Information theoretical analysis of quantum optimal control, Phys. Rev. Lett. **113**, 010502 (2014).
[29] P. Doria, T. Calarco, and S. Montangero, Optimal control technique for many-body quantum dynamics, Phys. Rev. Lett. **106**, 190501 (2011).
[30] S. van Frank, M. Bonneau, J. Schmiedmayer, S. Hild, C. Gross, M. Cheneau, I. Bloch, T. Pichler, A. Negretti, T. Calarco *et al.*, Optimal control of complex atomic quantum systems, Sci. Rep. **6**, 34187 (2016).
[31] I. Brouzos, A. I. Streltsov, A. Negretti, R. S. Said, T. Caneva, S. Montangero, and T. Calarco, Quantum speed limit and optimal control of many-boson dynamics, Phys. Rev. A **92**, 062110 (2015).
[32] S. Bera, A. Nazir, A. W. Chin, H. U. Baranger, and S. Florens, Generalized multipolaron expansion for the spin-boson model: Environmental entanglement and the biased two-state system, Phys. Rev. B **90**, 075110 (2014).
[33] N. Wu, L. Duan, X. Li, and Y. Zhao, Dynamics of the sub-Ohmic spin-boson model: A time-dependent variational study, J. Chem. Phys. **138**, 084111 (2013).
[34] N. Zhou, L. Chen, Y. Zhao, D. Mozyrsky, V. Chernyak, and Y. Zhao, Ground-state properties of sub-Ohmic spin-boson model with simultaneous diagonal and off-diagonal coupling, Phys. Rev. B **90**, 155135 (2014).
[35] N. Zhou, L. Chen, D. Xu, V. Chernyak, and Y. Zhao, Symmetry and the critical phase of the two-bath spin-boson model: Ground-state properties, Phys. Rev. B **91**, 195129 (2015).
[36] L. Wang, L. Chen, N. Zhou, and Y. Zhao, Variational dynamics of the sub-Ohmic spin-boson model on the basis of multiple Davydov D_1 states, J. Chem. Phys. **144**, 024101 (2016).
[37] Y. Zhao, The hierarchy of Davydov's ansätze: From guesswork to numerically "exact" many-body wave functions, J. Chem. Phys. **158**, 080901 (2023).
[38] L. Chen, Y. Yan, M. F. Gelin, and Z. Lü, Dynamics of the spin-boson model: The effect of bath initial conditions, J. Chem. Phys. **158** (2023).
[39] A. J. Leggett, S. Chakravarty, A. T. Dorsey, M. P. A. Fisher, A. Garg, and W. Zwerger, Dynamics of the dissipative two-state system, Rev. Mod. Phys. **59**, 1 (1987).
[40] K. Le Hur, Entanglement entropy, decoherence, and quantum phase transitions of a dissipative two-level system, Ann. Phys. (Amsterdam) **323**, 2208 (2008).
[41] R. Bulla, N.-H. Tong, and M. Vojta, Numerical renormalization group for bosonic systems and application to the sub-Ohmic spin-boson model, Phys. Rev. Lett. **91**, 170601 (2003).
[42] P. P. Orth, D. Roosen, W. Hofstetter, and K. Le Hur, Dynamics, synchronization, and quantum phase transitions of two dissipative spins, Phys. Rev. B **82**, 144423 (2010).
[43] S. Bera, S. Florens, H. U. Baranger, N. Roch, A. Nazir, and A. W. Chin, Stabilizing spin coherence through environmental entanglement in strongly dissipative quantum systems, Phys. Rev. B **89**, 121108(R) (2014).
[44] U. Weiss, *Quantum Dissipative Systems* (World Scientific, Singapore, 2012).
[45] B. Peropadre, D. Zueco, D. Porras, and J. J. García-Ripoll, Nonequilibrium and nonperturbative dynamics of ultrastrong coupling in open lines, Phys. Rev. Lett. **111**, 243602 (2013).
[46] F. Yoshihara, T. Fuse, S. Ashhab, K. Kakuyanagi, S. Saito, and K. Semba, Superconducting qubit-oscillator circuit beyond the ultrastrong-coupling regime, Nat. Phys. **13**, 44 (2017).
[47] P. Forn-Díaz, J. J. García-Ripoll, B. Peropadre, J.-L. Orgiazzi, M. Yurtalan, R. Belyansky, C. M. Wilson, and A. Lupascu, Ultrastrong coupling of a single artificial atom to an electromagnetic continuum in the nonperturbative regime, Nat. Phys. **13**, 39 (2017).
[48] L. Magazzù, P. Forn-Díaz, R. Belyansky, J.-L. Orgiazzi, M. Yurtalan, M. R. Otto, A. Lupascu, C. Wilson, and M. Grifoni, Probing the strongly driven spin-boson model in a superconducting quantum circuit, Nat. Commun. **9**, 1403 (2018).
[49] M. Marcuzzi, J. c. v. Minář, D. Barredo, S. de Léséleuc, H. Labuhn, T. Lahaye, A. Browaeys, E. Levi, and I. Lesanovsky, Facilitation dynamics and localization phenomena in Rydberg lattice gases with position disorder, Phys. Rev. Lett. **118**, 063606 (2017).
[50] F. M. Gambetta, W. Li, F. Schmidt-Kaler, and I. Lesanovsky, Engineering nonbinary Rydberg interactions

via phonons in an optical lattice, Phys. Rev. Lett. **124**, 043402 (2020).
[51] H. Tamura, T. Yamakoshi, and K. Nakagawa, Analysis of coherent dynamics of a Rydberg-atom quantum simulator, Phys. Rev. A **101**, 043421 (2020).
[52] R. V. Skannrup, R. Gerritsma, and S. Kokkelmans, Phonon-mediated spin-spin interactions between trapped Rydberg atoms, arXiv:2008.13622 (2020).
[53] P. Méhaignerie, C. Sayrin, J.-M. Raimond, M. Brune, and G. Roux, Spin-motion coupling in a circular Rydberg state quantum simulator: Case of two atoms, Phys. Rev. A **107**, 063106 (2023).
[54] D. F. V. James, Quantum dynamics of cold trapped ions with application, Appl. Phys. B **66**, 181 (1998).
[55] D. Porras and J. I. Cirac, Bose-Einstein condensation and strong-correlation behavior of phonons in ion traps, Phys. Rev. Lett. **93**, 263602 (2004).
[56] C. Schneider, D. Porras, and T. Schaetz, Experimental quantum simulations of many-body physics with trapped ions, Rep. Prog. Phys. **75**, 024401 (2012).
[57] D. Kienzler, H.-Y. Lo, B. Keitch, L. De Clercq, F. Leupold, F. Lindenfelser, M. Marinelli, V. Negnevitsky, and J. Home, Quantum harmonic oscillator state synthesis by reservoir engineering, Science **347**, 53 (2015).
[58] H.-Y. Lo, D. Kienzler, L. de Clercq, M. Marinelli, V. Negnevitsky, B. C. Keitch, and J. P. Home, Spin-motion entanglement and state diagnosis with squeezed oscillator wavepackets, Nature (London) **521**, 336 (2015).
[59] D. Kienzler, H.-Y. Lo, V. Negnevitsky, C. Flühmann, M. Marinelli, and J. P. Home, Quantum harmonic oscillator state control in a squeezed Fock basis, Phys. Rev. Lett. **119**, 033602 (2017).
[60] Q.-X. Mei, B.-W. Li, Y.-K. Wu, M.-L. Cai, Y. Wang, L. Yao, Z.-C. Zhou, and L.-M. Duan, Experimental realization of the Rabi-Hubbard model with trapped ions, Phys. Rev. Lett. **128**, 160504 (2022).
[61] D. Lv, S. An, Z. Liu, J.-N. Zhang, J. S. Pedernales, L. Lamata, E. Solano, and K. Kim, Quantum simulation of the quantum Rabi model in a trapped ion, Phys. Rev. X **8**, 021027 (2018).
[62] M.-L. Cai, Z.-D. Liu, W.-D. Zhao, Y.-K. Wu, Q.-X. Mei, Y. Jiang, L. He, X. Zhang, Z.-C. Zhou, and L.-M. Duan, Observation of a quantum phase transition in the quantum Rabi model with a single trapped ion, Nat. Commun. **12**, 1126 (2021).
[63] See Supplemental Material at http://link.aps.org/supplemental/10.1103/PhysRevLett.132.170401 for the details of the (i) non-Gaussian *Ansatz*, (ii) scaling and adiabaticity analysis of the state preparation protocols, and (iii) realization of the model with trapped ions, which includes Refs. [11,14,21,33,36,38–41,43,61,62,64–76].
[64] A. V. Kirkova, D. Porras, and P. A. Ivanov, Out-of-time-order correlator in the quantum Rabi model, Phys. Rev. A **105**, 032444 (2022).
[65] J. Pedernales, I. Lizuain, S. Felicetti, G. Romero, L. Lamata, and E. Solano, Quantum Rabi model with trapped ions, Sci. Rep. **5**, 15472 (2015).
[66] J. Roland and N. J. Cerf, Quantum search by local adiabatic evolution, Phys. Rev. A **65**, 042308 (2002).
[67] J. W. Britton, B. C. Sawyer, A. C. Keith, C.-C. J. Wang, J. K. Freericks, H. Uys, M. J. Biercuk, and J. J. Bollinger, Engineered 2D Ising interactions on a trapped-ion quantum simulator with hundreds of spins, Nature (London) **484**, 489 (2012).
[68] M. L. Wall, A. Safavi-Naini, and A. M. Rey, Boson-mediated quantum spin simulators in transverse fields: X Y model and spin-boson entanglement, Phys. Rev. A **95**, 013602 (2017).
[69] D. Leibfried, R. Blatt, C. Monroe, and D. Wineland, Quantum dynamics of single trapped ions, Rev. Mod. Phys. **75**, 281 (2003).
[70] R. Puebla, M.-J. Hwang, J. Casanova, and M. B. Plenio, Probing the dynamics of a superradiant quantum phase transition with a single trapped ion, Phys. Rev. Lett. **118**, 073001 (2017).
[71] A. E. Webb, S. C. Webster, S. Collingbourne, D. Bretaud, A. M. Lawrence, S. Weidt, F. Mintert, and W. K. Hensinger, Resilient entangling gates for trapped ions, Phys. Rev. Lett. **121**, 180501 (2018).
[72] Y. Shapira, J. Markov, N. Akerman, A. Stern, and R. Ozeri, Programmable quantum simulations on a trapped-ions quantum computer with a global drive, arXiv:2308.16036.
[73] C. Rackauckas and Q. Nie, Differentialequations.jl–a performant and feature-rich ecosystem for solving differential equations in JULIA, J. Open Res. Software **5**, 15 (2017).
[74] P. K. Mogensen and A. N. Riseth, Optim: A mathematical optimization package for JULIA, J. Open Source Software **3**, 615 (2018).
[75] S. Krämer, D. Plankensteiner, L. Ostermann, and H. Ritsch, Quantumoptics. jl: A JULIA framework for simulating open quantum systems, Comput. Phys. Commun. **227**, 109 (2018).
[76] X. Yuan, S. Endo, Q. Zhao, Y. Li, and S. C. Benjamin, Theory of variational quantum simulation, Quantum **3**, 191 (2019).
[77] P. Kramer and M. Saraceno, Geometry of the time-dependent variational principle in quantum mechanics, in *Group Theoretical Methods in Physics: Proceedings of the IX International Colloquium Held at Cocoyoc, México, 1980* (Springer, New York, 2005), pp. 112–121.
[78] E. Leviatan, F. Pollmann, J. H. Bardarson, D. A. Huse, and E. Altman, Quantum thermalization dynamics with matrix-product states, arXiv:1702.08894.
[79] A. Hallam, J. Morley, and A. G. Green, The Lyapunov spectra of quantum thermalisation, Nat. Commun. **10**, 2708 (2019).
[80] A. A. Michailidis, C. J. Turner, Z. Papić, D. A. Abanin, and M. Serbyn, Slow quantum thermalization and many-body revivals from mixed phase space, Phys. Rev. X **10**, 011055 (2020).
[81] C. J. Turner, J.-Y. Desaules, K. Bull, and Z. Papić, Correspondence principle for many-body scars in ultracold Rydberg atoms, Phys. Rev. X **11**, 021021 (2021).
[82] M. Serbyn, D. A. Abanin, and Z. Papić, Quantum many-body scars and weak breaking of ergodicity, Nat. Phys. **17**, 675 (2021).

[83] M.-J. Hwang, R. Puebla, and M. B. Plenio, Quantum phase transition and universal dynamics in the Rabi model, Phys. Rev. Lett. **115**, 180404 (2015).
[84] Z.-J. Ying, M. Liu, H.-G. Luo, H.-Q. Lin, and J. Q. You, Ground-state phase diagram of the quantum Rabi model, Phys. Rev. A **92**, 053823 (2015).
[85] M. Gärttner, J. G. Bohnet, A. Safavi-Naini, M. L. Wall, J. J. Bollinger, and A. M. Rey, Measuring out-of-time-order correlations and multiple quantum spectra in a trapped-ion quantum magnet, Nat. Phys. **13**, 781 (2017).
[86] M. Gärttner, P. Hauke, and A. M. Rey, Relating out-of-time-order correlations to entanglement via multiple-quantum coherences, Phys. Rev. Lett. **120**, 040402 (2018).
[87] R. Lewis-Swan, A. Safavi-Naini, J. J. Bollinger, and A. M. Rey, Unifying scrambling, thermalization and entanglement through measurement of fidelity out-of-time-order correlators in the Dicke model, Nat. Commun. **10**, 1581 (2019).
[88] This has motivated the design of alternative protocols such as in [89].
[89] K. Agarwal, R. N. Bhatt, and S. L. Sondhi, Fast preparation of critical ground states using superluminal fronts, Phys. Rev. Lett. **120**, 210604 (2018).
[90] A. Omran, H. Levine, A. Keesling, G. Semeghini, T. T. Wang, S. Ebadi, H. Bernien, A. S. Zibrov, H. Pichler, S. Choi *et al.*, Generation and manipulation of Schrödinger cat states in Rydberg atom arrays, Science **365**, 570 (2019).
[91] T. Caneva, T. Calarco, and S. Montangero, Chopped random-basis quantum optimization, Phys. Rev. A **84**, 022326 (2011).
[92] P. Richerme, C. Senko, J. Smith, A. Lee, S. Korenblit, and C. Monroe, Experimental performance of a quantum simulator: Optimizing adiabatic evolution and identifying many-body ground states, Phys. Rev. A **88**, 012334 (2013).
[93] Here the gap refers to the distance to the first excited state in the same parity sector as the ground state.
[94] A. Lucas, Quantum many-body dynamics on the star graph, arXiv:1903.01468.
[95] T. Guaita, L. Hackl, T. Shi, C. Hubig, E. Demler, and J. I. Cirac, Gaussian time-dependent variational principle for the Bose-Hubbard model, Phys. Rev. B **100**, 094529 (2019).
[96] R. Menu and T. Roscilde, Gaussian-state ansatz for the non-equilibrium dynamics of quantum spin lattices, SciPost Phys. **14**, 151 (2023).
[97] M. P. Kaicher, D. Vodola, and S. B. Jäger, Mean-field treatment of the long-range transverse field Ising model with fermionic Gaussian states, Phys. Rev. B **107**, 165144 (2023).
[98] C. H. Valahu, V. C. Olaya-Agudelo, R. J. MacDonell, T. Navickas, A. D. Rao, M. J. Millican, J. B. Pérez-Sánchez, J. Yuen-Zhou, M. J. Biercuk, C. Hempel, T. R. Tan, and I. Kassal, Direct observation of geometric-phase interference in dynamics around a conical intersection, Nat. Chem. **15**, 1503 (2023).
[99] H. R. Grimsley, S. E. Economou, E. Barnes, and N. J. Mayhall, An adaptive variational algorithm for exact molecular simulations on a quantum computer, Nat. Commun. **10**, 3007 (2019).
[100] O. R. Meitei, B. T. Gard, G. S. Barron, D. P. Pappas, S. E. Economou, E. Barnes, and N. J. Mayhall, Gate-free state preparation for fast variational quantum eigensolver simulations, npj Quantum Inf. **7**, 155 (2021).
[101] B. de Neeve, T.-L. Nguyen, T. Behrle, and J. P. Home, Error correction of a logical grid state qubit by dissipative pumping, Nat. Phys. **18**, 296 (2022).
[102] V. A. *et al.*, Quantum error correction zoo (2023), https://errorcorrectionzoo.org/.
[103] H. Weimer, A. Kshetrimayum, and R. Orús, Simulation methods for open quantum many-body systems, Rev. Mod. Phys. **93**, 015008 (2021).
[104] R. Puebla, A. Smirne, S. F. Huelga, and M. B. Plenio, Universal anti-Kibble-Zurek scaling in fully connected systems, Phys. Rev. Lett. **124**, 230602 (2020).
[105] D. S. Schlegel, F. Minganti, and V. Savona, Coherent-state ladder time-dependent variational principle for open quantum systems, arXiv:2306.13708.
[106] N. A. Kamar and M. Maghrebi, Hybrid quantum-classical stochastic approach to spin-boson models, arXiv:2309.11553.
[107] N. A. Kamar, D. A. Paz, and M. F. Maghrebi, Spin-boson model under dephasing: Markovian vs non-Markovian dynamics, arXiv:2305.00110.
[108] L. Bond, B. Gerritsen, J. Minář, R. Gerritsma, and A. Safavi-Naini, Open dynamics with non-Gaussian variational ansatz for ion cooling (to be published).
[109] M. Cerezo, A. Arrasmith, R. Babbush, S. C. Benjamin, S. Endo, K. Fujii, J. R. McClean, K. Mitarai, X. Yuan, L. Cincio, and P. J. Coles, Variational quantum algorithms, Nat. Rev. Phys. **3**, 625 (2021).